SCANNER OBSERVATIONS OF COMET WILSON (1986 (1))

By B. B. Sanwal and B. S. Rautela
Uttar Pradesh State Observatory

An estimate of the CN, C_2 and C_3 abundances and their production rates have been made from the spectrophotometric scans of the head of Comet Wilson.

1. *Introduction*

Comet Wilson (1986 (1)) was discovered by Christine Wilson[1] on plates taken with the 1·2-m Schmidt telescope at Palomar. The comet appeared diffuse with some condensation and an apparent short tail to the south-east. Many observers since reported the total visual magnitude of the comet on many nights. Larson & Levy[2] reported, on the basis of spectra taken on September 2·3 and 3·3 UT, that the comet showed a strong dust continuum and *CN* (388 nm) emission and direct *CCD* images showed a well-defined and asymmetric dust coma and jet-like features. Ducati & Costa[3] obtained photoelectric photometry of the comet and showed on the basis of the ratios of intensities of molecular bands to neighbouring continuum, an increase in CO^+ emission of 35 per cent in the outer coma, and emission from C_2 also increased outward by 80 per cent. Emissions from C_3 and H_2O^+ had constant strength over the observed region. Tail disconnection was observed by Garradd[4] on photographs taken on April 20·8 UT. Brook *et al.*[5] detected emission features at 2·8 and 3·8 μm on May 24 using the NASA Infrared Telescope Facility. The band positions and shapes closely resembled the unidentified emission features discovered in the spectrum of P/Halley in 1986. Larson *et al.*[6] detected water vapour using high resolution infrared spectra acquired with the University of Arizona's Fourier Transform Spectrometer on NASA's Kuiper Airborne Observatory. The water production rate was about 2 to 3×10^{29} molecules s^{-1}. *OH* emission from this comet was observed by Gerard *et al.*[7] and Palmer *et al.*[8] whilst *HCN* was observed by Crovisier *et al.*[9] with radio telescopes.

We observed Comet Wilson to estimate the abundance of different molecular species and their production rates from the emission features in the visible region.

2. *Observations*

The comet was observed on four nights with a spectrum scanner, mounted at the Cassegrain focus (f/13) of the 104-cm reflector. A circular diaphragm of 3 mm corresponding to 45 arcseconds as projected on the sky and centred on the nucleus of the comet was used. The basic parameters of the comet for the days of the observations are given in Table I. The scanner consists of a Hilger & Watts monochromator giving a dispersion of 70 Å mm^{-1} in the first order. The exit slot of 50 Å band pass, in the first order, was used. The detector was a cooled (−20°C) EMI 9658 B photomultiplier. Standard d.c. techniques were employed for recording. Scans of the neighbouring sky taken before and after each scan of the comet enabled elimination of the contribution by the background sky.

The standard star α Leo was observed to check the wavelength calibration of the scanner, and to standardize the observations of the comet. The observations were corrected for atmospheric extinction and were reduced to absolute values. The absolute values of the fluxes thus obtained correspond to Taylor's[10] calibration of α Lyr. The absolute flux distribution of the comet for four nights is shown in Fig. 1.

3. Molecular Emission Bands

The prominent emission features, as can be seen in Fig. 1, are CN ($\Delta V = 0$) at 388·3 nm, C_2 ($\Delta V = +1, 0, -1$) at 469·5, 516·5 and 553·8 nm respectively. Weak emission features due to $CH+C_3$ at 405 nm and C_2 ($\Delta V = -2$) at 619 nm are also

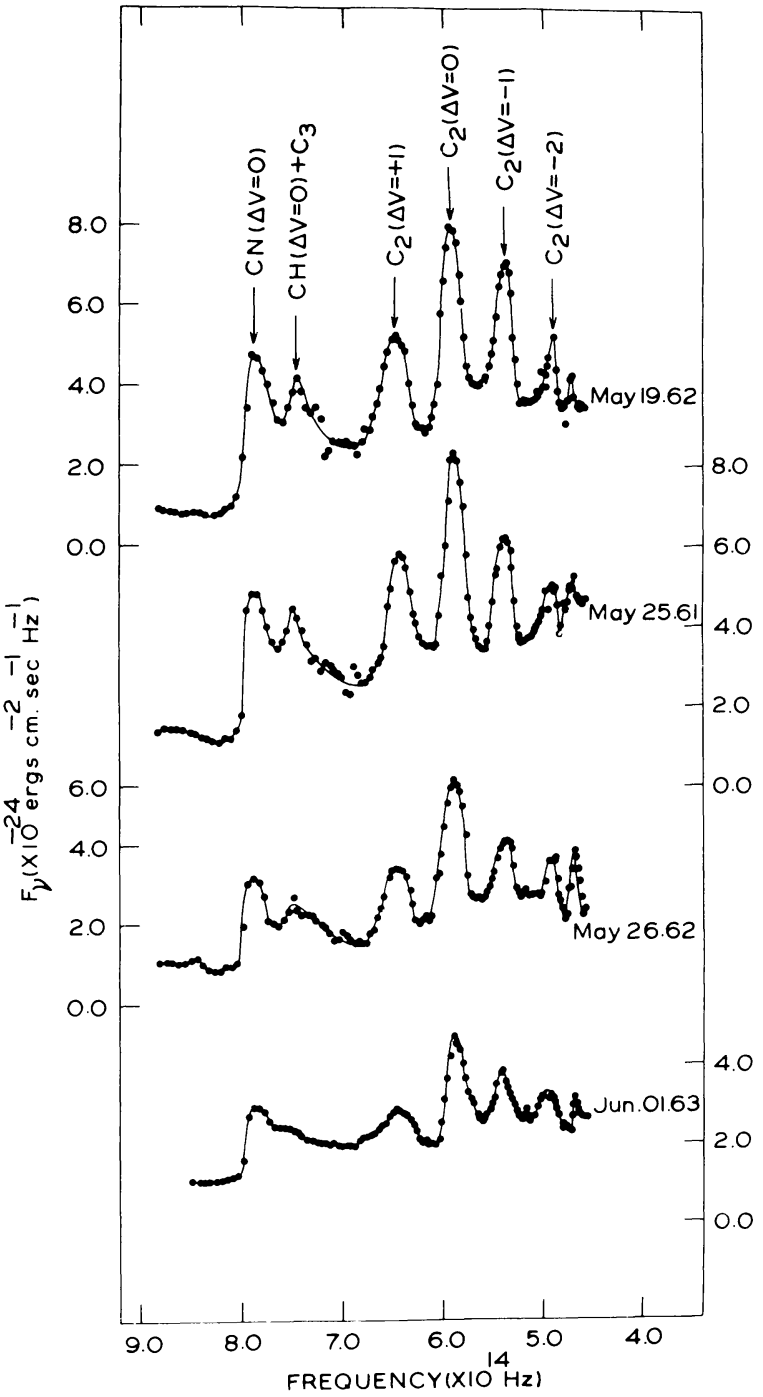

FIG. 1

Absolute flux distribution of the head of Comet Wilson (1986 (1)).

present. The C_2 ($\Delta V = 0$) emission is the strongest feature in the whole spectrum. The heliocentric distances of the comet, during the period of our observations, were more than 1·28 AU and a comet generally displays sodium emission when its heliocentric distance is less than 0·8 AU as shown by Bappu & Sivaraman[11]. Thus, as expected, no trace of the *Na* D line (589 nm) was detected. In order to measure fluxes in the emission bands, the continuum in the spectrum was located by selecting wavelength regions free of emission lines. The area of the strong emission bands was measured and converted into the total flux. Emission band fluxes relative to C_2 (516 nm) are listed in Table II. The observed flux and the total luminosity for C_2 (516 nm) band sequence are also given in Table II.

4. Column Densities and Production Rates

The number of molecules of each observed species, contained in a cylinder of radius defined by the diaphragm used and extending entirely through the coma was evaluated using the standard formula by Millis *et al.*[12]:

$$\log M(\varrho) = \log F(\varrho) + 27{\cdot}449 + 2\log(\Delta \cdot r) - \log g$$

where F is the observed flux in cgs units, r and Δ are the heliocentric and geocentric distances of the comet respectively in AU, and g the fluorescence efficiency (in cgs units) per molecule at 1 AU. We used the values of the fluorescence efficiency for C_2 and C_3 from Sivaraman *et al.*[13]. Because of the Swings effect, g (CN) varies significantly with the comet's heliocentric radial velocity. Orbital elements for the comet were taken from *IAU Circular No.* 4364 to calculate the radial velocity. During our observations the radial velocity varied from 9·3 to 12·4 km s^{-1} and the value of g was obtained from the figure of Tatum & Gillespie[14]. The column densities obtained are listed in Table III.

The column densities thus calculated were converted into production rates, Q, assuming a Haser model, through the relationship given by A'Hearn & Cowan[15]:

$$M(\varrho) = QV^{-1}\varrho\left[\int_x^{\mu x} K_0(y)dy + (1/x)(1 - 1/\mu) + K_1(\mu x) - K_1(x)\right]$$

where V is the velocity of released species; μ is the ratio between daughter and parent molecules scale lengths; K_0 and K_1 are modified Bessel functions of the second kind of order 0 and 1. Following Delsemme[16] we assumed $V = 0.58/\sqrt{r}$. The parent and daughter scale lengths were taken from Cochran[17]. Bessel functions were calculated using the tables of Abramowitz & Stegun[18] and the extrapolation formulae therein. The resulting production rates are given in Table III. Production rates for dust have been estimated on the simplest possible model–spherically symmetric, uniform outflow ignoring variations in particle sizes, scattering angle, etc. The relationship derived by A'Hearn & Cowan[15] was used to evaluate the production rate, Q, of dust in arbitrary units.

$$Q = const.\ L\, r^2/\varrho$$

where L is the luminosity of the comet at $\lambda = 485{\cdot}0$ nm and *const.* = 1. The dust production rates evaluated are listed in Table III.

5. Results

The production rates (s^{-1}) of the various molecular species *versus* the comet–Sun distance have been plotted in Fig. 2. The production rate of dust (arbitrary units) is also plotted in the same Figure. The straight lines are the linear best fits by eye judgement. We find that the production rate, for the three species considered,

varies with solar distance as usual but the large outburst in C_2 and C_3 production on May 25 is remarkable. This outburst subsided on May 26 and did not occur in *CN*. The difference in slopes for *CN*, C_2 and C_3 is insignificant. The ratio of the production rate of *CN* to the production rate of C_2 is found to be equal to $0{\cdot}43\pm0{\cdot}08$, which is of the same order as given by A'Hearn *et al.*[19]. There are no systematic variations in dust production rates with comet–Sun distance. A'Hearn & Cowan[15] also observed a similar large outburst in C_2 production in Comet Kohoutek. They tried to decide whether the outburst is a phenomenon totally internal to the comet or is triggered by an external source such as the Sun and concluded that both possibilities are equally plausible.

The solar X-ray and optical flux increased on May 24 and 25 as reported in the Solar Geophysical Data. We feel that this evidence makes the possibility of solar triggering more plausible for the outburst in C_2 and C_3 production on May 25.

References

(1) C. Wilson, *IAU Circ. No.* 4241, 1986.
(2) S. Larson & D. Levy, *IAU Circ. No.* 4243, 1986.
(3) J. R. Ducati & R. D. D. Costa, *IAU Circ. No.* 4375, 1987.
(4) G. Garradd, *IAU Circ. No.* 4375, 1987.
(5) T. Brooke, R. Knacke, T. Owen & A. Tokunage, *IAU Circ. No.* 4399, 1987.
(6) H. P. Larson, M. J. Mumma, H. A. Weaver & S. Drapatz, *IAU Circ. No.* 4403, 1987.
(7) E. Gerard, D. Bockelee-Morvan, G. Bourgois, P. Colom & J. Crovisier, *IAU Circ. No.* 4271, 1986.
(8) P. Palmer, I. de Pater & L. Snyder, *IAU Circ. No.* 4314, 1987.
(9) J. Crovisier, D. Despois, D. Bockelee-Morvan & E. Gerard, *IAU Circ. No.* 4411, 1987.
(10) B. J. Taylor, *Ap. J. Suppl.*, **54**, 259, 1984.
(11) M. K. V. Bappu & K. R. Sivaraman, *Solar Phys.*, **10**, 496, 1969.

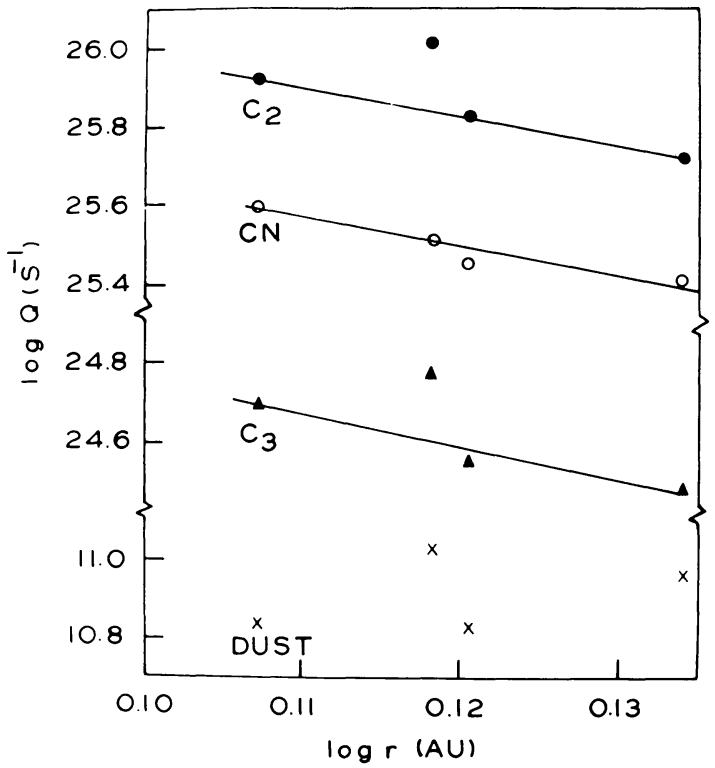

FIG. 2

The production rates of C_2, *CN*, C_3 molecules and dust as a function of heliocentric distance.

Table I

Basic data of Comet Wilson

Date (UT) 1987	*Geocentric distance (Δ) AU*	*Heliocentric distance (r) AU*	*Predicted m_1*	*Radius of circular region in the sky at Δ (10^4 km)*	*Area of sky at Δ admitted through diaphragm ($km^2 \times 10^8$)*
May 19·622	0·911	1·280	5·3	1·49	6·97
May 25·613	1·078	1·313	5·8	1·76	9·73
May 26·619	1·107	1·320	5·9	1·81	10·29
June 01·625	1·292	1·361	6·4	2·11	13·99

Table II

Observed fluxes of emission bands relative to $C_2(\Delta V = 0)$

Date (UT)	*Apparent flux $F(C_2 \Delta V = 0)$ (ergs cm^{-2} s^{-1})$\times 10^{-10}$*	*$F/F(C_2, \Delta V = 0)$*						
		$CN(\Delta V = 0)$	*$CH(\Delta V = 0)$ + $C_3(\Delta V = 0)$*	*$C_2(\Delta V = 1)$*	*$C_2(\Delta V = 0)$*	*$C_2 = (\Delta V = -1)$*	*$C_2(\Delta V = -2)$*	*Luminosity (L) of $C_2(\Delta V = 0)$ (erg s^{-1})$\times 10^{17}$*
May 19·622	1·23	0·813	0·724	0·675	1·000	0·626	0·187	2·87
May 25·613	1·14	0·781	0·746	0·655	1·000	0·491	0·178	3·73
May 26·619	0·84	0·704	0·595	0·583	1·000	0·456	0·171	2·89
June 01·625	0·60	0·770	0·575	0·517	1·000	0·424	0·179	2·82

Table III

Column densities (M) and production rates (Q)

Date (UT) 1987	*Log (M)*					*Log (Q)*			
	$CN(\Delta V = 0)$	*$C_2(\Delta V = 1)$*	*$C_2(\Delta V = 0)$*	*$C_2(\Delta V = -1)$*	*$C_3(\Delta V = 0)$*	*$CN(\Delta V = 0)$*	*$C_2(\Delta V = 0)$*	*$C_3(\Delta V = 0)$*	*dust*
May 19·622	29·806	30·122	30·027	30·151	29·356	25·60	25·92	24·70	10·84
May 25·613	29·933	30·274	30·163	30·181	29·504	25·51	26·01	24·77	11·03
May 26·619	29·890	30·089	30·058	29·966	29·301	25·45	25·82	24·55	10·83
June 01·625	29·956	30·036	30·058	30·012	29·307	25·41	25·72	24·48	10·96

(12) R. L. Millis, M. F. A'Hearn & D. T. Thompson, *A.J.*, **87**, 1310, 1982.
(13) K. R. Sivaraman, G. S. D. Babu, B. S. Shylaja & R. Rajmohan, *A. & A.*, **187**, 543, 1987.
(14) J. B. Tatum & M. L. Gillespie, *Ap. J.*, **218**, 569, 1977.
(15) M. F. A'Hearn & J. J. Cowan, *A.J.*, **80**, 852, 1975.
(16) A. H. Delsemme, *Comets* (University of Arizona, USA), p. 85, 1982.
(17) A. L. Cochran, *A.J.*, **90**, 2609, 1985.
(18) M. Abramowitz & I. A. Stegun, *Handbook of Mathematical Functions*, NBS Appl. Math. Ser., Washington, D.C., No. 55, 1964.
(19) M. F. A'Hearn, R. L. Millis & P. V. Birch, *A.J.*, **84**, 570, 1979.

MAGNITUDE CALIBRATION IN THE CORDOBA ATLAS

By Maria V. Alonso and J. L. Sersic
Observatorio Astronomico, Universidad Nacional de Cordoba, Argentina

The total magnitudes given in the *Atlas de Galaxies Australes*[1] for more than 50 southern hemisphere objects are referred to a provisional zero point, due to the lack of photoelectric data at that time.

In the present note we give:

Zero points, resulting from the calibration of the photographic isophotes with photoelectric observations taken from Longo & de Vaucouleurs[3].

Total magnitudes, resulting from new planimetry of the isophotal contours in the *Atlas* and a new, more objective, extrapolation procedure.

Mean magnitudes in de Vaucouleurs' system[4,5].

The foregoing analysis was performed for 36 galaxies with suitable photoelectric observations. Finally, all the magnitudes given in the *Atlas* were reduced to de Vaucouleurs' system.

The basic integration procedure followed to compute the magnitudes in the provisional scale is described by Sersic[1,2]. The circles representing the diaphragms of the photoelectric observations were drawn on the maps of isophotes. It was assumed that all diaphragms were centred on the nucleus. The magnitude, in the provisional scale, corresponding to each diaphragm was then integrated. It was necessary to measure the areas of isophotes several times (between 3 and 6) for 3 to 9 diaphragms on each galaxy. The photoelectric B-values provided us with an estimate of the magnitude of the zero point for each galaxy. A simple average of these estimates was then used as the photoelectric zero point for the given galaxy. Its *r.m.s.* error will be used later to compute the relative weight of the corresponding total magnitude.

Surface photographic photometry in the *Atlas* was not extended to levels low enough to warrant a suitable extrapolation leading to total magnitudes. So we have constructed the curve IS from the isophotal areas $S(m)$ and their intensities against the magnitude m, as defined in reference 2. We have computed, consequently, the luminosity $L(m_1)$ up to the last measured isophote and then applied a completeness correction as follows: let us define the variable x as in Sersic[2],

$$x = 0{\cdot}921\ (m_1 - m_N) + N \qquad (1)$$

where m_N is the magnitude corresponding to the maximum $I_N S_N$ in the curve IS *vs* m (see Fig. 1), N is an integer and the function $E_N(y) = \sum_{j=0}^{N} y^j/j!$. It has been shown[2] that the relationship between $L(m)$, the luminosity up to the limit magnitude m, and the total luminosity L_T can be written as

$$L(m) = L_T(1 - E_{N-1}(x)\ \exp(-x)).$$